

Research Article

# Advancing brain drug delivery: Focused magnetic hyperthermia and magnetic particle imaging for real-time BBB modulation

Hafiz Ashfaq Ahmad<sup>a,†</sup>, Hohyeon Kim<sup>a,†</sup>, Ji-Hye Kim<sup>b</sup>, Kang-Ho Choi<sup>b,\*</sup>, Jungwon Yoon<sup>a,\*</sup>

<sup>a</sup>School of Integrated Technology, Gwangju Institute of Science and Technology, Gwangju, South Korea

<sup>b</sup>Department of Neurology, Chonnam National University Medical School and Hospital, Gwangju, South Korea

<sup>†</sup>Contributed equally

\*Corresponding author, email: [jyoon@gist.ac.kr](mailto:jyoon@gist.ac.kr), [ckhchoikang@hanmail.net](mailto:ckhchoikang@hanmail.net)

Received 29 November 2024; Accepted 20 August 2025; Published online 29 August 2025

© 2025 Ahmad *et al.*; licensee Infinite Science Publishing GmbH

This is an Open Access article distributed under the terms of the Creative Commons Attribution License (<http://creativecommons.org/licenses/by/4.0>), which permits unrestricted use, distribution, and reproduction in any medium, provided the original work is properly cited.

## Abstract

The blood-brain barrier (BBB) is crucial for brain protection but limits therapeutic delivery for neurological disorders. This study utilizes magnetic hyperthermia (MH) to transiently and reversibly open the BBB, with magnetic particle imaging (MPI) enabling real-time, high-sensitivity monitoring. Using field-free point (FFP)-based focused heating, MH facilitated magnetic nanoparticles (MNPs) penetration into the brain and prolonged retention in the target area. Fluorescence imaging was confirmed on Evans blue staining to analyze BBB permeability immediately after MH, while MPI quantification revealed significant MNPs accumulation at target sites in focused-heated groups compared to non-heated controls. Fluorescence images further showed that BBB permeability restored after 24 hours, though MNPs retention persisted in heated regions for more than 72 hours. Fluorescence imaging confirms BBB permeability immediately after MH, while MPI provides both qualitative imaging and quantitative data on MNPs distribution and retention. These findings indicate that MPI can detect particle retention and distribution patterns that are not visible with Fluorescence imaging.

## 1. Introduction

Magnetic nanoparticles (MNPs) have been utilized in various preclinical experiments, including targeted stimulation, drug delivery, and imaging [1]. MNPs accumulated in a specific area, and when alternating magnetic field is applied, it can enable localized heating [2]. This localized heating, achieved through field free point (FFP), has emerged as a promising method for transiently and reversibly altering the blood-brain barrier (BBB) which serves as a sentinel, shielding the brain from harmful substances but also impeding the entry of many life-saving drugs [3, 4]. Overcoming this barrier is critical for ad-

vancing treatments for conditions such as brain cancer, neurodegenerative diseases, and stroke [5]. While BBB permeability changes have traditionally been confirmed through biopsies, real-time monitoring remains a challenge [6].

Magnetic particle imaging (MPI) offers exceptional sensitivity and specificity for tracking MNPs *in vivo*, enabling real-time visualization of their distribution and concentration [7]. Combined with magnetic particle spectroscopy (MPS), these techniques allow precise quantification of MNPs and prediction of BBB changes in living subjects. BBB permeability was assessed by quantifying the fluorescence intensity of Evans blue extrav-

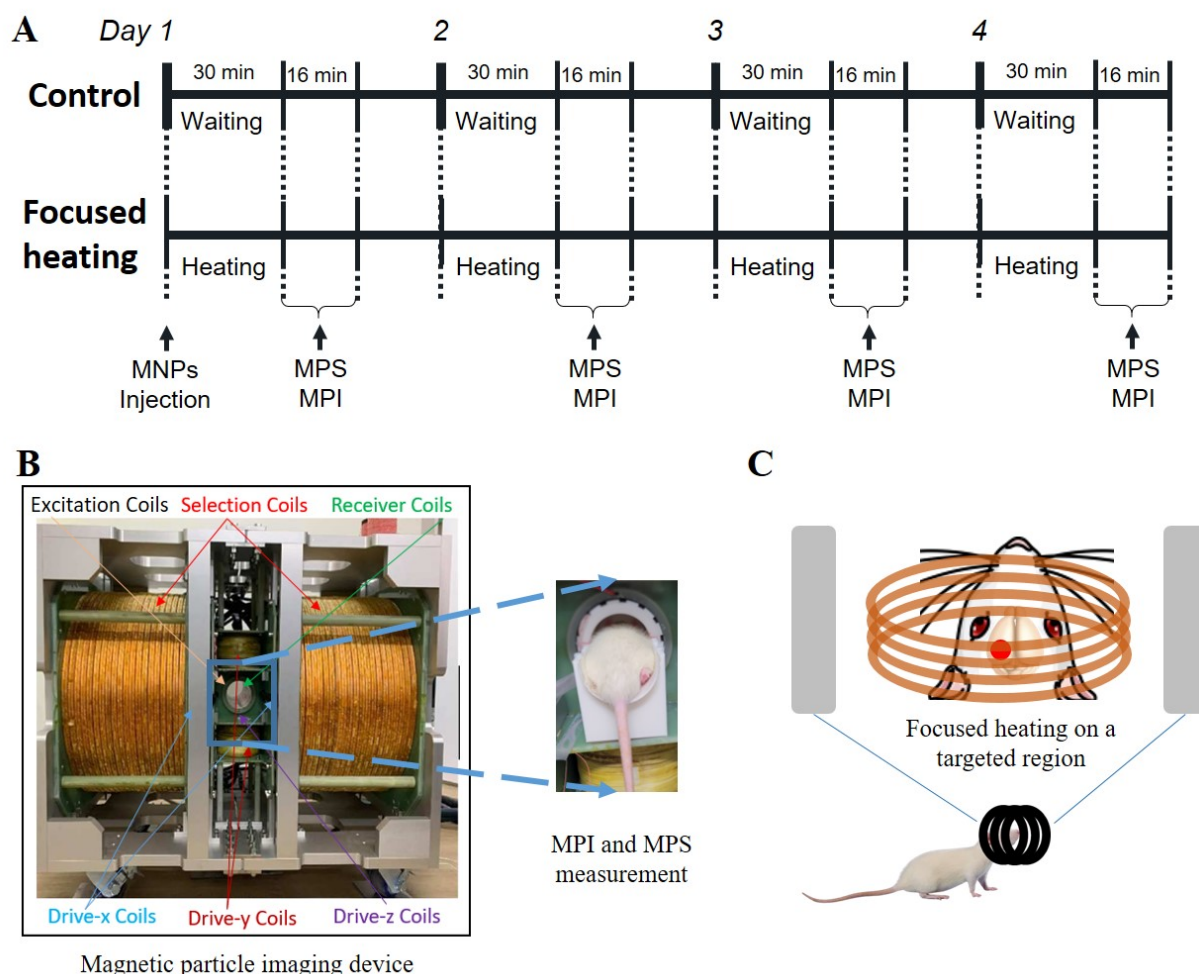


**Figure 1:** Experimental design and protocol for control and focused heating groups. (A) Timeline showing MNPs injection, periodic MPI/MPS measurements, and focused heating sessions. (B) MPI device and in vivo setup for imaging and quantification. (C) Illustration of focused heating targeting specific brain regions to modulate BBB permeability.

sation using an *in vivo* imaging system (IVIS) to confirm BBB disruption *in vivo* [8]. As a result, particle accumulation at the target site was confirmed, along with confirmation of BBB permeability changes and the feasibility of repeated hyperthermia.

## II. Materials and Methods

In this study, we investigated changes in particle accumulation due to focused heating, which were quantified using MPS and MPI signals, while the effects on BBB permeability were assessed by comparing groups with and without heating.

The experiment was conducted on twenty-four 8-week-old Sprague-Dawley (SD) rats using two different particle concentrations of Synomag<sup>®</sup> (micromod, Germany) magnetic nanoparticles (30 mg/mL and 15 mg/mL, used volume is 60  $\mu$ L). A complete experimen-

tal design and protocol is shown in Figure 1. The rats were divided into two groups: Focused heating group underwent injection, 30-minute focused heating, and lab-made MPS/MPI measurement, while control group involved injection, a 30-minute wait, and MPS/MPI measurement by using the MPI device [9]. All rats were anesthetized with 3% isoflurane during the experiment and were returned to their cages afterward. MPI and MPS measurements were performed for each rat at 0.5, 24, 48, and 72 hours. FFP-based focused heating was generated by gradient magnetic field of two permanent magnets [10]. MNPs were injected into the internal carotid artery (ICA) of the rat to achieve direct access to the brain [5]. Figure 1A illustrates the experimental timeline: for focused heating, MNPs were injected, followed by 30 minutes of focused heating at the targeted brain region. The heating area, including the subcortical region such as the striatum, was selected to validate results as an extension of a previous experiment conducted in a

**Table 1:** Mass estimation of *in vitro* samples using MPS/MPI quantification. The table compares original and estimated MNPs masses ( $\mu\text{g}$ ) across five samples, with errors ranging between 2.08% and 5.22%.

Sample	Original ( $\mu\text{g}$ )	Estimated ( $\mu\text{g}$ )	Error (%)
1	18.6	19.35	4.04
2	18.6	18.19	2.19
3	18.6	19.57	5.21
4	50	47.60	4.78
5	100	97.92	2.08

disease model [5]. Then, MPS/MPI measurements were performed, as shown in Figure 1B. The focused heating was conducted for 30 minutes under a gradient field of 2.1 T/m. An alternating magnetic field (AMF) with an amplitude of 7 mT<sub>rms</sub> and a frequency of 595.4 kHz was applied, see Figure 1C. The effective heating area, confirmed through theoretical calculations and phantom testing, was determined to be 3.5 mm. A custom head holder was designed and used to consistently target the same brain region in all rats. For the control group, after the injection, rats were kept waiting for 30 minutes before MPS/MPI measurements, ensuring measurements were conducted at the same time point for both groups.

MPS measurements were performed using the same device by activating only the excitation and receiver channels, capturing stable real-time signals for one minute. Following MPS, 3D MPI images of the rat's head were acquired for all rats. This protocol allowed MPS and MPI measurements to be conducted 30 minutes' post-injection for both groups to assess the effect of focused heating on the targeted region.

Changes in BBB permeability due to localized heating were confirmed by injecting Evans Blue into the tail vein immediately after magnetic hyperthermia. When BBB permeability increases, Evans Blue leaks into the affected area, allowing for quantitative evaluation of BBB disruption. This leakage was assessed using a IVIS. IVIS images were obtained from brains extracted immediately after focused heating and again after 24 hours. The focused heating setup is illustrated in Figure 1C.

The MPS and MPI signals accurately quantified particle concentrations using a validated technique confirmed through controlled sample studies. Five samples were prepared: Samples 1–3, containing 18.9  $\mu\text{g}$  of iron, varied in volume (87  $\mu\text{L}$ , 174  $\mu\text{L}$ , and 261  $\mu\text{L}$ ) and concentration (0.217 mg/mL, 0.109 mg/mL, and 0.072 mg/mL, respectively). Sample 4 (50  $\mu\text{g}$  of iron) and Sample 5 (100  $\mu\text{g}$  of iron) were both 87  $\mu\text{L}$ , with concentrations of 0.575 mg/mL and 1.15 mg/mL, respectively. These samples validated the quantification technique for mass estimation.

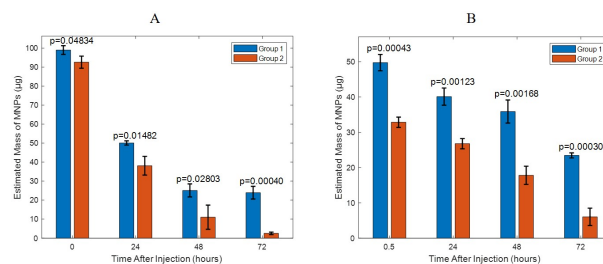


**Figure 2:** MPS results showing significant differences in MNPs retention between groups, with focused heating group retaining particles longer than control group over 72 hours. (A) is for 30 mg/mL concentrations and (B) is for 15 mg/mL.

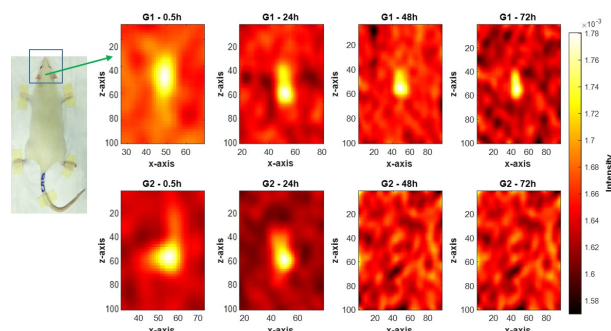


**Figure 3:** MPI images of focused heating group and control group with concentration 15 mg/mL at 0.5, 24, 48, and 72 hours post-injection. Focused heating group shows sustained MNPs accumulation at the target region, while control group displays MNPs dispersion over time.

### III. Results and discussion

Before commencing *in vivo* measurements, MPS and MPI signals were evaluated using *in vitro* samples of known concentrations, quantified through the mass estimation technique [11, 12]. Table 1 highlights the precision of MPS and MPI in estimating particle mass, showing errors within a range of 2.08% to 5.22%. These findings confirm the reliability and accuracy of MPI quantification methods based on *in vitro* validation studies.

The MPS signals measured 30 minutes after magnetic thermal stimulation and at 24, 48, and 72 hours demonstrated significant differences (p-value < 0.05) between groups with and without focused heating (Figure 2). These findings indicate that thermal stimulation enhances particle retention in the targeted brain region. In focused heating group, MNPs remained in the target area significantly longer than in control group, underscoring the role of thermal stimulation in promoting localized particle accumulation. Notably, this effect was observed across both concentrations (30 mg/mL and 15 mg/mL), highlighting the efficacy of thermal magnetic stimulation in sustaining MNPs retention compared to the control group.

**Table 2:** Estimated MNP mass ( $\mu\text{g}$ ) from MPI measurements over time. Heating group shows higher retention at the target region compared to control group, with significant differences observed.

MPI Measurement Time	Estimated MNPs mass from MPI Results ( $\mu\text{g}$ )			
	15 mg/mL		30 mg/mL	
	Focused heating	Control	Focused heating	Control
After 0.5 hours	44.71	27.16	60.92	47.63
After 24 hours	26.37	10.82	37.56	26.08
After 48 hours	19.08	5.731	18.82	7.52
After 72 hours	16.71	2.161	17.92	1.88

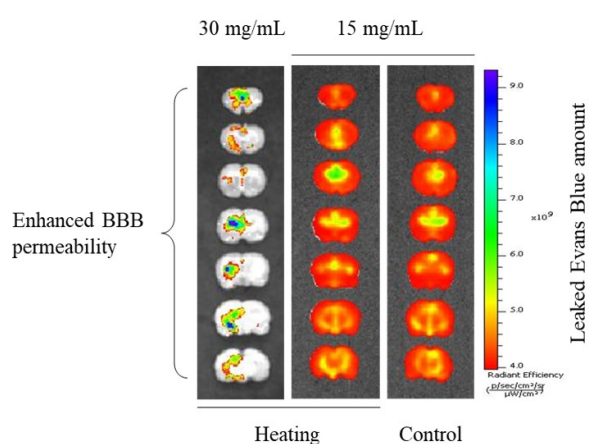


**Figure 4:** IVIS image of rat brain showing BBB permeability. The left slice (30 mg/mL MNPs) shows a higher BBB permeability, while the middle slice (15 mg/mL MNPs) shows non-significant changes in BBB permeability compared to the control (right slice).

Figure 3 presents MPI images of each groups at 15 mg/mL concentration, taken at 0.5, 24, 48, and 72 hours' post-injection. In focused heating group, MNPs demonstrated sustained accumulation at the target region, remaining localized even after 72 hours. In contrast, control group exhibited progressive dispersion of MNPs over time, with noticeable redistribution by 48 hours due to systemic circulation. These results highlight the role of focused magnetic hyperthermia in enhancing MNPs retention at the target site. Initial particle accumulation in the target area is driven by the gradient field, and the increased temperature from targeted heating of particles in the surrounding region ultimately enhances BBB permeability. This localized increase in permeability allows nanoparticles to cross the BBB within the targeted area; However, additional experiments may be required to evaluate the long-term effects of the particles within brain tissue.

Table 2 quantifies the estimated mass of MNPs in the

rat brain using partial field of view (pFOV) visualization and quantification of MPI measurements [13]. MPS and MPI results confirms that thermal stimulation increased BBB permeability even at 15 mg/mL which was previously not detected by other modalities [3].

BBB permeability was confirmed via IVIS imaging (Figure 4) after thermal stimulation at a concentration of 30 mg/mL. However, BBB permeability was restored after 24 h, suggesting that BBB changes may only be estimated from early IVIS images [5]. The heat generated at a particle concentration of 15 mg/mL was sufficient to demonstrate therapeutic effects, such as motor function recovery and inflammation reduction [3, 5], but was insufficient to confirm BBB opening using Evans blue. Consequently, no significant change in BBB permeability was observed compared to the control group, regardless of whether heating was applied. In focused heating group at 30 mg/mL, BBB changes were observed in IVIS, and particle accumulation was confirmed in MPI and MPS. On the other hand, in the condition of 15 mg/mL concentration that had a therapeutic effect, BBB changes were not statistically confirmed in IVIS, but significant particle accumulation was still confirmed in MPI. Even at a concentration of 15 mg/mL, the initially injected particle dose is relatively high; however, it becomes diluted upon entering the bloodstream, suggesting that optimized injection concentrations may be necessary for applications in primates or humans with larger total blood volumes and vessel sizes.

Although high concentrations may pose a risk of tissue damage, magnetic hyperthermia has been shown to safely and transiently modulate BBB permeability [5], and the expression of tight junction proteins in the experimental group indicated enhanced BBB integrity through the restoration of endothelial function [3]. Our study demonstrated the potential to estimate BBB opening if temperature data could be obtained from accurate particle estimations using MPI prior to therapeutic delivery [10, 14]. Focused magnetic hyperthermia effectively delivered thermal energy to the target site. This precise modulation was validated in this study, where real-time MPI imaging confirmed targeted MNP retention, underscoring the potential of MPI and focused magnetic hyperthermia as minimal invasive methods for brain-targeted therapy.

Our experimental results suggest that focused magnetic heating can be applied to alter BBB permeability. However, the effects of targeted brain heat delivery require more detailed evaluation. In particular, when aiming to enhance drug delivery efficiency, it is important to distinguish between the effects of localized brain stimulation and those resulting from increased BBB permeability. Since these effects depend on the temperature at the target region, additional experiments are essential to estimate it using MPI. As a preliminary step toward *in vivo* temperature estimation, heat generation at the lesion



site was simulated to predict the temperature rise, and the actual increase was validated using iron oxide particle samples with the same concentration. However, image-based information is critical for MPI applications, and achieving temperature estimation through MPI imaging remains a key goal for future research.

## IV. Conclusions

This study establishes MPI as a powerful non-invasive tool for real-time monitoring of BBB dynamics and precise quantification of MNPs distribution *in vivo*. Magnetic hyperthermia was demonstrated to transiently enhance BBB permeability, enabling sustained MNPs retention at the target site. While higher nanoparticle concentrations (30 mg/mL) effectively induced BBB modulation, lower concentrations (15 mg/mL) showed limited impact on BBB permeability despite detectable MPI signals. Our findings indicate that MPI can detect particle retention and distribution patterns that are not visible with IVIS imaging, highlighting its superior sensitivity for monitoring MNPs behavior *in vivo*. These results emphasize the importance of optimizing nanoparticle dosage and thermal stimulation parameters to maximize therapeutic efficacy for brain-targeted applications. MPI's ability to provide both qualitative (visualization of particle localization and retention) and quantitative (precise estimation of particle mass and distribution) insights represents a promising advancement in developing safe, effective methods for localized brain therapies.

## Author's statement

The authors presented this work under the same title and with the same abstract at IWMPi 2025. Conflict of interest: Authors state no conflict of interest.

## Acknowledgments

This research was funded by the National Research Foundation of Korea (NRF) grant, and Government of Korea (MSIT) with grant no. RS-2025-00554248.

## References

- [1] M. Roet, S.-A. Heschem, A. Jahanshahi, B. P. Rutten, P. O. Anikeeva, and Y. Temel. Progress in neuromodulation of the brain: A role for magnetic nanoparticles? *Progress in Neurobiology*, 177:1–14, 2019, doi:[10.1016/j.pneurobio.2019.03.002](https://doi.org/10.1016/j.pneurobio.2019.03.002).
- [2] H. Gavilán, S. K. Avugadda, T. Fernández-Cabada, N. Soni, M. Cassani, B. T. Mai, R. Chantrell, and T. Pellegrino. Magnetic nanoparticles and clusters for magnetic hyperthermia: optimizing their heat performance and developing combinatorial therapies to tackle cancer. *Chemical Society Reviews*, 50(20):11614–11667, 2021, doi:[10.1039/D1CS00427A](https://doi.org/10.1039/D1CS00427A).
- [3] J.-H. Kim, M. Jeong, H. Kim, J.-H. Kim, J. W. Ahn, B. Son, K.-H. Choi, S. Chung, and J. Yoon. Focused magnetic stimulation for motor recovery after stroke. *Brain Stimulation*, 17(5):1048–1059, 2024, doi:[10.1016/j.brs.2024.08.011](https://doi.org/10.1016/j.brs.2024.08.011).
- [4] S. N. Tabatabaei, H. Girouard, A.-S. Carret, and S. Martel. Remote control of the permeability of the blood–brain barrier by magnetic heating of nanoparticles: A proof of concept for brain drug delivery. *Journal of Controlled Release*, 206:49–57, 2015, doi:[10.1016/j.jconrel.2015.02.027](https://doi.org/10.1016/j.jconrel.2015.02.027).
- [5] H. Kim, J. Kim, J. Kim, S. Oh, K. Choi, and J. Yoon. Magnetothermal-based non-invasive focused magnetic stimulation for functional recovery in chronic stroke treatment. *Scientific Reports*, 13(1):4988, 2023, doi:[10.1038/s41598-023-31979-w](https://doi.org/10.1038/s41598-023-31979-w).
- [6] K. J. Chung, Y. G. Abdelhafez, B. A. Spencer, T. Jones, Q. Tran, L. Nardo, M. S. Chen, S. Sarkar, V. Medici, V. Lyo, R. D. Badawi, S. R. Cherry, and G. Wang. Quantitative PET imaging and modeling of molecular blood–brain barrier permeability, 2024. doi:[10.1101/2024.07.26.24311027](https://doi.org/10.1101/2024.07.26.24311027).
- [7] C. Lu, L. Han, J. Wang, J. Wan, G. Song, and J. Rao. Engineering of magnetic nanoparticles as magnetic particle imaging tracers. *Chemical Society Reviews*, 50(14):8102–8146, 2021, doi:[10.1039/D0CS00260G](https://doi.org/10.1039/D0CS00260G).
- [8] D. J. Lundy, K.-J. Lee, I.-C. Peng, C.-H. Hsu, J.-H. Lin, K.-H. Chen, Y.-W. Tien, and P. C. H. Hsieh. Inducing a Transient Increase in Blood–Brain Barrier Permeability for Improved Liposomal Drug Therapy of Glioblastoma Multiforme. *ACS Nano*, 13(1):97–113, 2019, doi:[10.1021/acsnano.8b03785](https://doi.org/10.1021/acsnano.8b03785).
- [9] T.-A. Le, M. P. Bui, and J. Yoon. Development of Small-Rabbit-Scale Three-Dimensional Magnetic Particle Imaging System With Amplitude-Modulation-Based Reconstruction. *IEEE Transactions on Industrial Electronics*, 70(3):3167–3177, 2023, doi:[10.1109/TIE.2022.3169715](https://doi.org/10.1109/TIE.2022.3169715).
- [10] T.-A. Le, Y. Hadadian, and J. Yoon. A prediction model for magnetic particle imaging–based magnetic hyperthermia applied to a brain tumor model. *Computer Methods and Programs in Biomedicine*, 235:107546, 2023, doi:[10.1016/j.cmpb.2023.107546](https://doi.org/10.1016/j.cmpb.2023.107546).
- [11] A. Dinari, H. Ashfaq Ahmad, M. P. Bui, S. Oh, Y.-H. Kim, D.-H. Kim, and J. Yoon. Targeted Cellular Tracking of Pancreatic Cancer Cells via Magnetic Particle Spectroscopy (MPS). *Bio-Algorithms and Med-Systems*, 20(Special Issue):63–70, 2024, doi:[10.5604/01.3001.0054.9363](https://doi.org/10.5604/01.3001.0054.9363).
- [12] A. Dinari, H. A. Ahmad, S. Oh, Y.-H. Kim, and J. Yoon. Advanced Detection of Pancreatic Cancer Circulating Tumor Cells Using Biomarkers and Magnetic Particle Spectroscopy. *Nanotheranostics*, 9(2):171–185, 2025, doi:[10.7150/ntno.110074](https://doi.org/10.7150/ntno.110074).
- [13] J. J. Gevaert, J. Konkle, P. Goodwill, and P. J. Foster. Multi-channel joint image reconstruction allows for artifact-free focused small field of view magnetic particle imaging, 2023. doi:[10.1101/2023.06.22.545970](https://doi.org/10.1101/2023.06.22.545970).
- [14] S. S. Natah, S. Srinivasan, Q. Pittman, Z. Zhao, and J. F. Dunn. Effects of acute hypoxia and hyperthermia on the permeability of the blood–brain barrier in adult rats. *Journal of Applied Physiology*, 107(4):1348–1356, 2009, doi:[10.1152/jappphysiol.91484.2008](https://doi.org/10.1152/jappphysiol.91484.2008).